

# Fabrication of Microspherical Catalyst with Hierarchical Porous Structure from Functional Monomers via Low-Temperature Phase-Separation Photopolymerization

KEMIN WANG AND LIFEI HE

<sup>1</sup> Biomedical Science and Technology Research Center, School of Mechatronic Engineering and Automation, Shanghai University, Shanghai 200444, PR China

<sup>2</sup> School of Materials Science and Engineering, Changzhou University, Changzhou, 213164, PR China

## ABSTRACT

*This study proposes a simple approach for the fabrication of microspherical catalysts with a hierarchical porous structure. The cross-linked porous microspheres with catalytic ability were prepared directly from small-molecular monomers via low-temperature phase-separation photopolymerization of water/oil suspension. The morphology, pore size, chemical structure, and thermal stability of the obtained porous microspheres were characterized by SEM, Mercury Intrusion Porosimetry, FTIR, and TGA. The porous microspheres directly served as an acid catalyst for the condensation reaction of benzaldehyde and ethylene glycol, which exhibited superior catalytic activity and recyclability. The results indicated that such porous microspheres have great potential in the application of acid catalysis.*

KEYWORDS: *Catalyst, Porous microspheres, Photopolymerization*

## INTRODUCTION

Porous polymer particles have attracted considerable interest and are widely applied in catalysis, drug carriers, biosensors, biomacromolecule separation, gas storage, chromatography and tissue engineering <sup>[1-7]</sup>

owing to its low density, large surface area, and excellent permeability <sup>[8]</sup>. In general, porous polymer microspheres could be fabricated by phase separation, porogen leaching, gas foaming, and colloidal templating <sup>[9-13]</sup>.

---

J. Polym. Mater. Vol. **36**, No. 3, 2019, 253-260

© Prints Publications Pvt. Ltd.

Correspondence author e-mail: kemin-wang@hotmail.com

DOI : <https://doi.org/10.32381/JPM.2019.36.03.5>

Porous microspheres were prepared by polymerization strategies with phase separation, including suspension, precipitation, emulsification polymerization and photopolymerization. Suspension polymerization is a heterogeneous polymerization process in which the monomer is mixed in a liquid matrix. The monomer or the mixture of monomer is insoluble in the liquid phase (such as water), hence forming drops within the liquid matrix. Suspension polymerization can only synthesize microporous polymer microspheres (5–1000  $\mu\text{m}$ ), the diameter and pore size of resulting microspheres being non-uniform [14]. Precipitation polymerization is similar to suspension polymerization. It initially begins as a homogeneous system in the continuous phase where the monomer and initiator are completely soluble, but upon initiation the formed polymer is insoluble and thus precipitates as a result of larger or less regular particles. Emulsification polymerization process involves the combination of solvents, emulsifiers, and surfactants where dispersed monomer droplets polymerize in a continuous solvent phase. Drawbacks of the process include high processing temperature, necessary for thermal polymerization and difficulties in removing additives in the polymer matrix.

Photopolymerization has several advantages including low energy consumption, solvent-free formulation, high polymerization speed [15–20], and can be performed at low temperatures (below 0°C). In previous studies, temperature induced phase separation of monomer solution and photopolymerization at low temperatures have been combined to produce crosslinked polymer monolith, microfibers, and microsphere

with hierarchical porous structure [21–23]. Those crosslinked polymers with controlled porous structures were synthesized directly from corresponding monomers and the whole process required no template, surfactant, or other additives. Moreover, this general way is applicable to all of the monomers that can be photopolymerized, thus paving the way for the fabrication of various functional entities.

Porous polymer microspheres were served only as scaffolds in the application of catalysts. The current study focuses on immobilization of functional agents or surface functionalization of microspheres to improve the catalytic effect [24–26]. In this study, a new method was proposed to produce porous polymeric microspheres with catalytic ability, by the combination of freezing suspension and low-temperature phase-separation photopolymerization. Compared with previous reports [27], the porous microspheres prepared on the basis of the catalytic functional monomer 2-acrylamide-2-methylpropanesulfonic acid (AMPS) can be directly used as an acid catalyst rather than as a scaffold for the catalyst. Hence, this study may provide a practical solution for the industry to make porous polymer microspheres as productive catalysts.

## MATERIALS AND METHOD

### Materials

Poly (ethylene glycol) diacrylate (PEGDA, molecular weight 600 g/mol) and 2-acrylamide-2-methylpropanesulfonic acid (AMPS) were purchased from Sigma-Aldrich (USA). The photoinitiator, 2-hydroxy-4-(2-hydroxyethoxy)-2-methyl propiophenone (2959), was purchased from BASF Schweiz AG (Switzerland). Cyclohexane, liquid paraffin, benzaldehyde, ethylene

glycol, sulfuric acid (H<sub>2</sub>SO<sub>4</sub>), p-toluenesulfonic acid (TsOH), and toluene were purchased from Qiangshen Regents (Jiangsu, China).

#### **Preparation of Cross-Linked Porous Polymeric Microspheres based on AMPS and PEGDA**

The preparation process of cross-linked porous polymeric microsphere is shown in Fig. 1. The water/oil suspension was initially formed under high-speed stirring (3000 rpm) with the continuous phase of hydrophobic liquid paraffin and the dispersed phase of aqueous solution containing AMPS monomer, cross-linker PEGDA, and 1 wt% photoinitiator 2959. Then the suspension was rapidly frozen in liquid nitrogen and treated at low temperature (-20°C) for 5 hours. The frozen suspension was next irradiated for 15 mins at -20°C by using a pointolite light source (OmniCure series 1000; wavelength range: 300-450 nm, light intensity = 100 mW/cm<sup>2</sup>) to solidify the photo-curable materials. The remaining paraffin and water were removed by the means of cyclohexane and ethanol extraction at low temperatures. Finally, the porous microspheres based on the crosslinking of AMPS and PEGDA were obtained.

#### **Catalytic Performance Test of Obtained Microspherical Catalyst**

For the catalytic performance test of the AMPS based porous microspheres, the condensation reaction of ethylene glycol and benzaldehyde was performed by stirring the mixture of the obtained porous microspheres (0.01 g), benzaldehyde (0.015 mol), ethylene glycol (0.015 mol), and cyclohexane (5 g) for 12 h at 90°C. Then the obtained liquid solution was analyzed by SHIMADZU GC-2010 Plus gas chromatograph (GC) equipped with a flame ionization detector working at 280°C and a 30 m RTX-1 column. The injected samples were heated from 160° to 200°C at a heating rate of 15°C/min. The catalytic performance tests for TsOH and sulfuric acid were also carried out under the same conditions for comparison. Moreover, to study the recyclability of the obtained microspherical catalysts, samples were washed three times with ethanol to remove the entire residue, dried under vacuum, and then reused for subsequent recycles under the same catalytic reaction conditions after the first cycle of catalytic performance test.

#### **Characterization**

The morphology of various microspheres was observed by SEM with the S-4700 (Hitachi) microscope. At least fifty microspheres from several SEM images were evaluated with the software Image J and an average diameter as well as a standard deviation was calculated.

FTIR spectra of AMPS monomer, PEGDA and obtained microspheres were recorded using a Nicolet iS5 Fourier transform infrared spectrometer (Thermo Fisher Scientific Inc.).

TGA was performed using a NETZSCH analyzer (TGA209F1D-0228-L) in nitrogen atmosphere.

Pore size distribution for the obtained microspheres were recorded by mercury intrusion porosimetry using a PostMaster-33 porosimeter.

## **RESULT AND DISCUSSION**

The low-temperature phase-separation photopolymerization of water/oil suspension was used to produce AMPS based porous microspherical catalysts (the experimental set-up is shown in Fig. 1). The aqueous solution of catalytic functional monomer AMPS and cross-linker PEGDA was added into hydrophobic liquid paraffin under high speed stirring to form a WATER/OIL suspension. This suspension was rapidly frozen by liquid nitrogen and was treated at low temperature (-20°C) for 5 hours in order to increase the double bond conversion of photo-curable monomers during low-temperature photopolymerization [23]. Polymeric microspheres based on the crosslinking of AMPS and PEGDA were obtained when the frozen suspension was irradiated by UV light. Water was then removed by low temperature solvent extraction; after which a mass of pores, inside and outside the microspheres were formed from the remaining spaces occupied by frozen solvent.

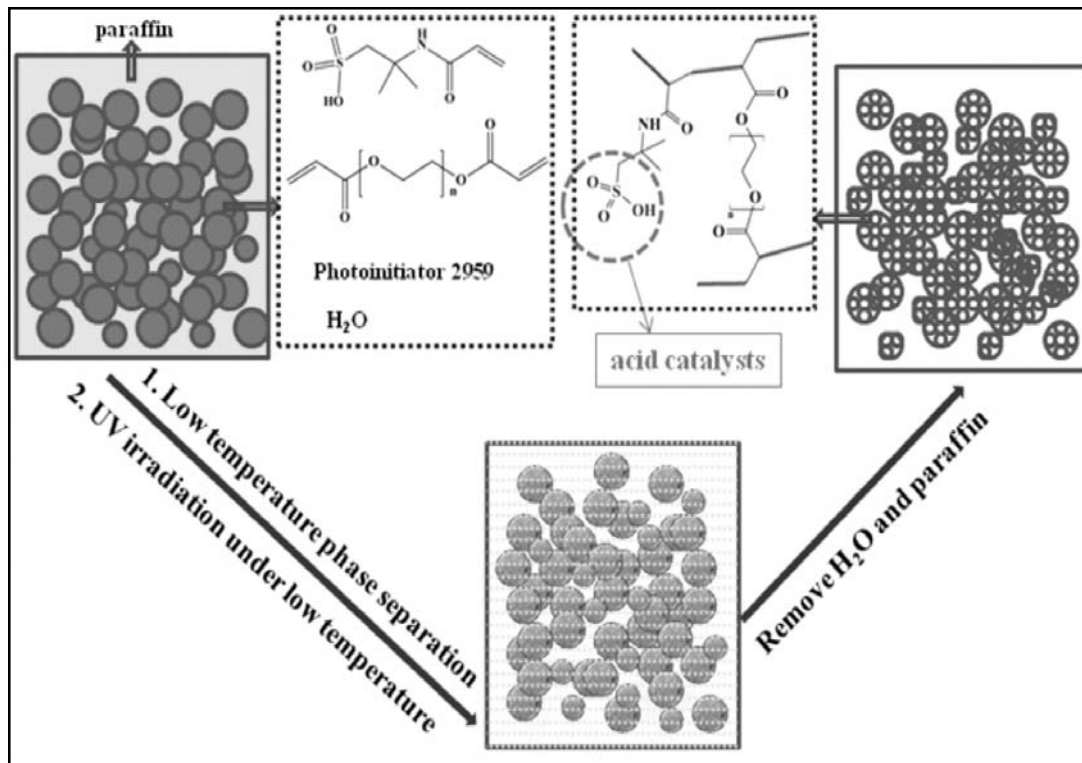


Fig. 1: Schematic representation of the preparation of porous polymeric microspheres by low-temperature phase-separation photopolymerization.

Figure 2 shows the morphology of the obtained porous microspherical catalysts formed by low temperature photopolymerization of AMPS and PEGDA containing the WATER/OIL suspension. The diameter of obtained microspheres was in the micro scale ranging from 10 to 140  $\mu\text{m}$  (Fig. 2A2-C2), with both the microsphere diameter and pore size being related to the AMPS concentration (Fig. 2 D and E). When the AMPS concentration increased from 4.3 to 14.4 wt%, the average diameter of microspheres reduced from 45 to 37  $\mu\text{m}$  (Fig. 2D). Such a reduction in diameter was mainly caused by the increase in viscosity

of the AMPS solution. The higher the liquid viscosity was, the smaller the droplets formed through WATER/OIL suspension; leading to the formation of microspheres with smaller sizes [28].

The pore number fraction determined from mercury intrusion measurements carried out at high pressure (Fig. 2E) revealed that the majority of the pore volume in the microspheres prepared at different AMPS concentrations was located in the macro pore range with the diameter between 10–45  $\mu\text{m}$ . It is also evident that with the increase of AMPS concentration from 4.3 to 14.4 wt%, the pore number fraction

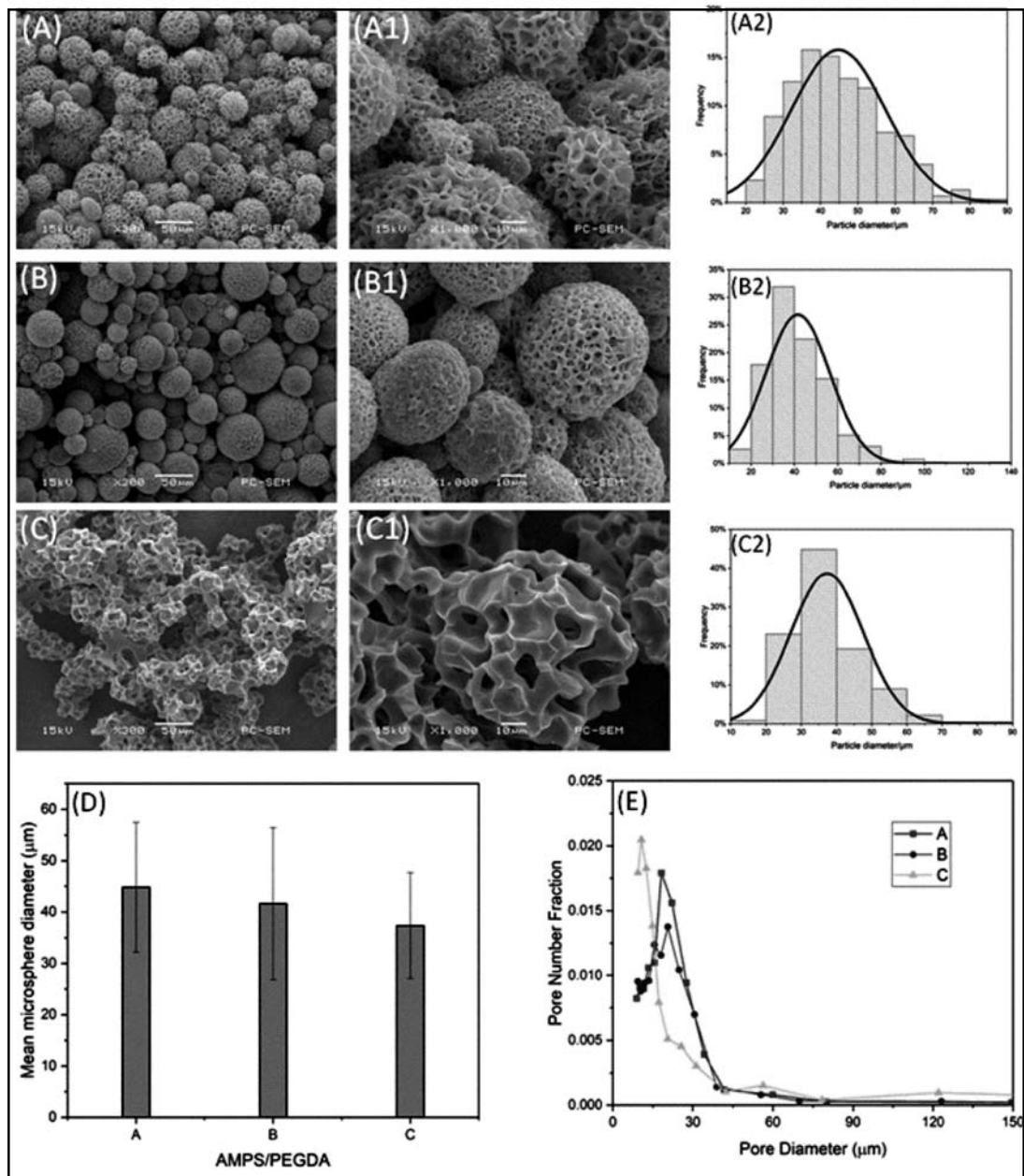


Fig. 2. SEM images of the obtained porous microspherical catalysts with low (A-C) and high (A1-C1) magnification at different AMPS and PEGDA concentrations: (A) AMPS = 4.3 wt%, PEGDA = 8.7 wt%; (B) AMPS = 12 wt%, PEGDA = 8 wt%; (C) AMPS = 14.4 wt%, PEGDA = 7.7 wt%; stirring speed = 3000 rpm and stirring time = 10 min; (A2-C2 and D) Diameter and (E) pore size distribution of the porous microspheres under different conditions.

of smaller pores increased and that of higher pores decreased. The reason behind this phenomenon could be that with higher concentration of AMPS solution, less crystallized ices disperse around the photopolymerized cross-linked polymers leading to the decrease of pore diameter in the microspheres.

The chemical structures of the catalytic functional monomer AMPS, the cross-linker PEGDA and the obtained crosslinked porous microspheres were studied by FTIR spectroscopy. Compared with the IR spectra of AMPS and PEGDA, the typical peak from the stretching and bending vibrations of C=CH group at  $810\text{ cm}^{-1}$  disappeared in the IR spectrum of the obtained porous microspheres, indicating the conversion of carbon-carbon double bonds in AMPS and PEGDA during low temperature photopolymerization.

The thermal stability of obtained porous microspherical catalysts was characterized by TGA. Fig. 3(2) shows that the initial thermal decomposition temperature was  $175^\circ\text{C}$ , and the weight loss of the microspheres obtained at different AMPS concentrations were 4.3, 12, and 14.4 wt%, respectively. It can also be seen from Fig. 3(2) that the maximum weight loss rate ( $T_{\text{max}}$ ) for three microspheres happen at  $225^\circ$ ,  $205^\circ$ , and  $219^\circ\text{C}$ , respectively. All of the microspherical catalysts prepared in this study have good thermal stability for further applications.

To test the catalytic performance of the obtained porous microspherical catalysts, the catalytic activity of the microspherical catalyst was compared with the common homogeneous acid catalysts TsOH and sulfuric acid in the catalysis of direct condensation reaction of benzaldehyde and ethylene glycol at  $90^\circ\text{C}$  for 12 h (Fig. 4(1)). With the catalysis of

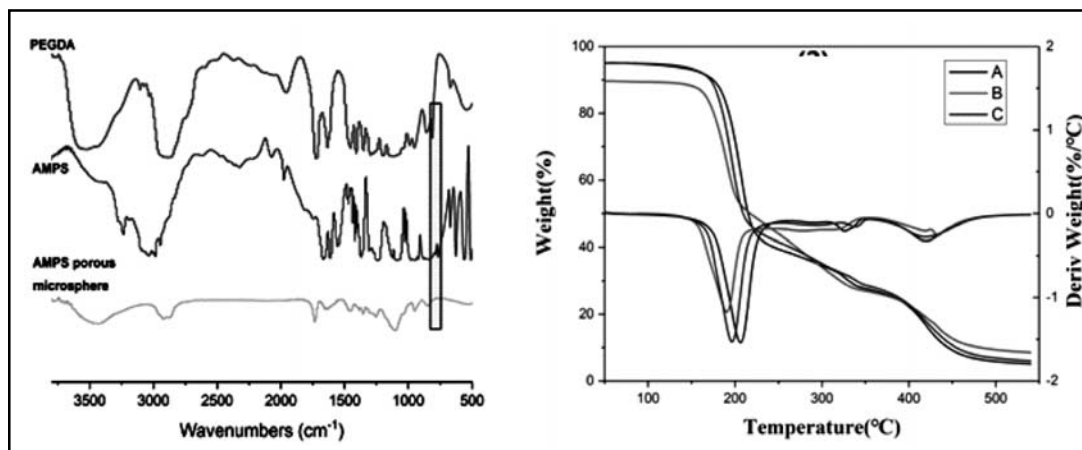


Fig. 3: (1) FT-IR spectra of catalytic functional monomer AMPS, the cross-linker PEGDA and the obtained crosslinked porous microspheres via low-temperature phase-separation photopolymerization. (2) TGA of the porous microspherical catalysts obtained from different AMPS and PEGDA concentrations: (A) AMPS = 4.3 wt%, PEGDA = 8.7 wt%; (B) AMPS = 12 wt%, PEGDA = 8 wt% and (C) AMPS = 14.4 wt%, PEGDA = 7.7 wt%.

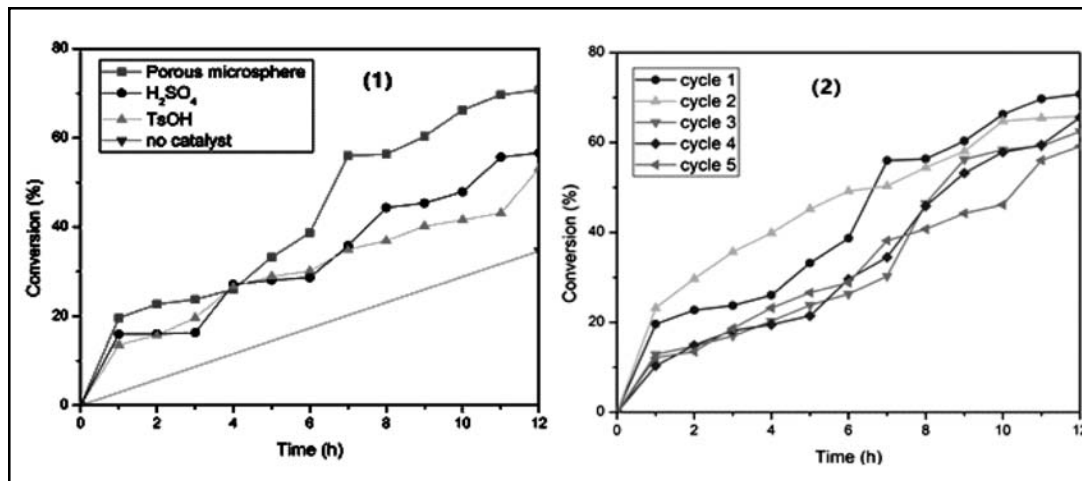


Fig. 4. (1) Comparison of the catalytic activity of obtained microspherical catalyst with the common homogeneous acid catalysts (TsOH and H<sub>2</sub>SO<sub>4</sub>) and no catalyst. (2) The recyclable catalytic ability of the porous microspherical catalysts after 5 cycles.

microspherical catalyst, the reaction proceeded smoothly to give benzaldehyde with 70% conversion, higher than the conversion catalyzed by TsOH and sulfuric acid (around 55%) and no catalyst. The cross-linked porous microspheres could not only produce H<sup>+</sup> as a catalyst, but also absorbed the generated water, causing the esterification reaction to move in the positive direction, leading to an increase in the reaction conversion. The recyclable catalytic ability of a catalyst, apart from its catalytic efficiency is another significant factor that should be taken into consideration for commercial applications. The recyclable catalytic ability of our porous microspherical catalysts is illustrated in Fig. 4(2). As expected, the conversion of benzaldehyde was around 70% for the first cycle and remains above 60% even after five catalytic cycles. The excellent catalytic ability of the porous microspherical catalysts might be attributed to the in situ inherited SO<sub>3</sub>H groups from AMPS monomers.

## CONCLUSIONS

In summary, this study opens up a simple approach for the direct fabrication of AMPS based porous microspherical catalysts by low-temperature phase-separation photopolymerization. The diameter of the obtained microspheres was in the micro scale ranging from 10 to 140 μm. The microspheres have hierarchical open porous structure and the majority of the pore volume was located in the macropore range with the diameter between 10–45 μm. The obtained AMPS based porous microspheres can be explored as an effective acid catalyst. The catalysis results exhibited significantly enhanced catalytic activity compared to common acid catalysts as well as excellent recyclability in the condensation reaction of benzaldehyde and ethylene glycol. Moreover, these porous microspheres may also find potential applications in controlled release, storage, gas sensing, and water purification.

## REFERENCES

1. J.A. Lee, Y.S. Nam, G.C. Rutledge, P.T. Hammond, *Adv. Funct. Mater.* 20, 2424-2429 (2010).
2. W. Liu, S. Thomopoulos, Y. Xia, *Adv. Healthc. Mater.* 1, 10-25 (2012).
3. D.A. Erdogan, M. Polat, R. Garifullin, M.O. Guler, E. Ozensoy, *Appl. Surf. Sci.* 308, 50-57 (2014).
4. X. Liu, X. Jin, P.X. Ma, *Nat. Mater.* 10, 398-406 (2011).
5. H. Xia, G. Wan, F. Yang, J. Wang, Q. Bai, *Mater. Lett.* 180, 19-22 (2016).
6. C.D. Wood, B. Tan, A. Trewin, F. Su, M.J. Rosseinsky, D. Bradshaw, Y. Sun, L. Zhou, A.I. Cooper, *Adv. Mater.* 20, 1916-1921 (2008).
7. J.B. Qu, Y.L. Xu, J.Y. Liu, J.B. Zeng, Y.L. Chen, W.Q. Zhou, J.G. Liu, *J. Chromatogr. A* 1441, 60-67 (2016).
8. C. Li, W. Wang, X. Wang, H. Jiang, J. Zhu, S. Lin, *Eur. Polym. J.* 68, 409-418 (2015).
9. Y.S. Nam, T.G. Park, *J. Biomed. Mater. Res.* 47, 8-17 (1999).
10. Y.S. Nam, T.G. Park, *Biomaterials* 20, 1783-1790 (1999).
11. Y.S. Nam, J.J. Yoon, T.G. Park, *J. Biomed. Mater. Res.* 53, 1-7 (2000).
12. Q. Hou, D.W. Grijpma, J. Feijen, *Biomaterials* 24, 1937-1947 (2003).
13. S.A. Johnson, P.J. Ollivier, T. E. Mallouk, *Science* 283, 963-965 (1999).
14. B. Yu, T. Xue, L. Pang, X. Zhang, Y. Shen, H. Cong, *Materials (Basel)* 11, 705 (2018).
15. F. Xu, J.-L. Yang, Y.-S. Gong, G.-P. Ma, J. Nie, *Macromolecules* 45, 1158-1164 (2012).
16. R. Shenoy, C.N. Bowman, *Macromolecules* 43, 7964-7970 (2010).
17. S.H. Dickens, J.W. Stansbury, K.M. Choi, C.J.E. Floyd, *Macromolecules* 36, 6043-6053 (2003).
18. Y. Yagci, S. Jockusch, N.J. Turro, *Macromolecules*, 43, 6245-6260 (2010).
19. C. Dietlin, S. Schweizer, P. Xiao, J. Zhang, F. Morlet-Savary, B. Graff, J.P. Fouassier, J. Lalevee, *Polym. Chem.* 6, 3895-3912 (2015).
20. P. Xiao, J. Zhang, F. Dumur, M.A. Tehfe, F. Morlet-Savary, B. Graff, D. Gigmes, J.P. Fouassier, J. Lalevee, *Prog. Polym. Sci.* 41, 32-66 (2015).
21. R. Yin, K. Wang, Y. Lu, J. Nie, *Macromol. Mater. Eng.* 300, 291-298 (2015).
22. K. Wang, J. Guan, F. Mi, J. Chen, H. Yin, J. Wang, Q. Yu, *Mater. Lett.* 161, 317-320 (2015).
23. K. Wang, L. He, S. Jiang, Q. Yu, *J. Polym. Mater.* 33, 753-758 (2016).
24. X. Wang, J. Gu, L. Tian, X. Zhang, *Sci. Rep.* 7, 44178 (2017).
25. J. Xu, G. Chen, R. Yan, D. Wang, M. Zhang, W. Zhang, P. Sun, *Macromolecules* 44, 3730-3738 (2011).
26. X. Ling, Y. Xie, X. Lin, L. Li, T. Qiu, *Chinese J. Chem. Eng.* In Press.
27. Y. Ning, Y. Yang, C. Wang, T. Ngai, Z. Tong, *Chem. Commun.* 49, 8761-8763 (2013).
28. J. Husny, J.J. Cooper-White, *J. Non-Newton. Fluid* 137, 121-136 (2006).

Received: 30-06-2019

Accepted: 04-09-2019